Advances in Science and Technology Research Journal

Advances in Science and Technology Research Journal 2022, 16(3), 295–305
https://doi.org/10.12913/22998624/150401
ISSN 2299–8624, License CC-BY 4.0

Received: 2022.04.12
Accepted: 2022.05.14
Published: 2022.06.01

# Optimization of Proportional-Integral Controllers of Grid-Connected Wind Energy Conversion System Using Grey Wolf Optimizer based on Artificial Neural Network for Power Quality Improvement

Fathi Abdulmajeed M. Alremali[1*], Ersagun Kürşat Yaylacı[1], İhsan Uluer[1]

[1] Department of Electrical and Electronic Engineering, Karabuk University, Karabuk, Turkey

* Corresponding author's email: fzhma2011@yahoo.com

**ABSTRACT**

This research presents a combination of artificial neural network (ANN) with the grey wolf optimizer (GWO) to improve the power quality of a grid-connected distributed power generation system (DPGS). To assess the effectiveness of the proposed algorithm, a grid-tied of small-scale wind energy conversion system (WECS) is chosen. The term power quality refers to voltage and frequency regulation, and limited harmonics. Power quality improvement is achieved through the cascaded control system's optimal tuning of three proportional-integral (PI) controllers of the grid-side inverter (GSI). However, because the DPGS model is computationally costly, the ANN model is utilized as an alternative model for DPGS. Furthermore, the ANN model is employed in conjunction with the GWO to boost the optimization precision and minimize the execution time of GWO. The considered power system was repetitively simulated to obtain the input-output datasets, which validate and train the ANN model. According to the ANN model's performance evaluation, the correlation coefficient (R) is close to one, while the mean squared error (MSE) is near zero. These findings demonstrate the ANN model's great accuracy in approximating the DPGS model. Using MATLAB/Simulink, the system's performance is evaluated using the optimum values obtained using GWO-ANN for various wind speed profiles. It showed the suggested power quality method's improved stability, convergence behavior, the effectiveness of the control mechanism, and the robustness of the proposed topology.

**Keywords:** artificial neural network, grey wolf optimizer, PI controller, grid connection, power quality, wind energy.

## INTRODUCTION

Wind energy is gaining popularity because it is a clean and sustainable energy source with minimal environmental impact. It also offers cost competitiveness, thanks to technological advancements [1]. The Global Wind Energy Council 2022 claims that there are currently over 837 GW cumulative wind power capacity installed worldwide [2]. Wind power's price stability makes it a viable and appealing option to other sources of renewable energy. As a result of the recent surge in the penetration of wind power plants into the grid [3], new grid regulations have been established by transmission system operators to ensure the steady and reliable operation of electric networks.

Active and reactive power regulation, fault ride-through capability, and power quality are all technological issues, that should be considered when integrating wind energy conversion systems (WECS) into the electrical network [4]. As a result, the operating parameters of WECS should be as close as possible to those of the utility grid to assure energy supply stability, dependability, and availability. Under normal situations, WECS should maintain a sinusoidal voltage within acceptable magnitude and frequency boundaries in terms of power quality. In addition, the harmonic and flicker emissions should be kept within the allowed limits [5]. The mismatch between the WECS and the utility grid's power quality parameters will result in poor supply quality [6].

The proposed DPGS in this study is a small-scale wind turbine consisting of a variable-speed wind turbine driving a directly-driven permanent magnet synchronous generator (DD-PMSG-VSWT). The considered power system has several benefits compared to constant-speed operations, including higher energy capture, operations at the maximum power point tracking (MPPT) for different wind speeds, decreased mechanical strains, reduced aerodynamic noise, and enhanced system reliability [7,8]. Due to a large number of rotor-pole pairs, the PMSG is ideal for a direct drive at low speeds [9]. The DD-PMSG-VSWT is connected to the grid via a frequency converter that consists of a grid-side inverter (GSI) and a machine-side converter (MSC) with a DC capacitor. However, usually, vector control is used for controlling both the MSC and GSI with numerous controllers like classical PI controllers (proportional-integral), fuzzy logic controller [10], sliding mode control [11], and feedback linearization [12], etc. The most widely used controllers are still PI regulators in the industry due to their resilience, ability, and long-term stability margins [13]. On the other hand, setting the PI controller's parameters, is cumbersome, especially in industrial systems with nonlinearities, high order, and delay time, therefore, the PI controller gains must be set correctly.

For fine-tuning PI regulator gain factors, many traditional and statistical methods are applied, including the Ziegler-Nichols method, Trial and Error method [14,15], Artificial Neural Network (ANN) [16], Taguchi technique [17], Cohen-Coon method [18], and Affine projection algorithm [19]. Unfortunately, the mentioned techniques are incapable of tuning higher-order, complex processes and are dependent on the incipient values [20,21]. Then there are meta-heuristic algorithms such as the Particle Swarm Optimization (PSO) [22], Differential Evolution Algorithm [23], Bee Algorithm [24], Whale Optimization Algorithm (WOA) [25], Genetic Algorithm [26], etc. that act as viable solutions for fine-tuning the PI controller parameters.

The Grey Wolf Optimizer (GWO) algorithm presented by Mirjalili [27] is a meta-heuristic method that was developed recently that imitates the grey wolves' community and their hunting dynamics. The GWO has sparked a lot of interest in medical, networking, environmental applications, bioinformatics, robotics, image processing, machine learning, control engineering, and electric power engineering [28]. Researchers have successfully applied the GWO algorithm to the PID controller design [29]. In research [30], the GWO algorithm is used to manage load frequency. The authors of previous research [31] used GWO for a magnetic levitation system for optimizing a proportional integral derivative (PID) controller whereas, in another work, the researchers proposed the GWO algorithm for a DC-DC boost converter for tuning PID controller parameters. Using GWO, the PI controller has been successfully tuned in the pitch angle control system for tuning a fixed-speed wind turbine [32]. Authors of another research [33,34] used both GWO and PSO for control parameter optimization of MSC and GSI for improving the double-fed induction generator-based VSWT system's transient operation, which proved the efficiency of the proposed algorithm. Recently GWO's performance was benchmarked concerning exploitation, exploration, convergence, and local optima avoidance on unimodal, multimodal, fixed-dimension multimodal, and composite functions [27]. It has been shown a significant advantage over other well-known meta-heuristics in that only a few control parameters must be modified [35].

However, the DD-PMSG-VSWT system has a computational complexity, which is certainly a drawback in the case of direct application of the optimization algorithms to the power system especially when a large number of iterations are applied to the GWO algorithm. Hence, the authors could be thought the considered power system model is approximated using an ANN model as an alternative to cope with this drawback and decrease the computational time and enhance the optimization accuracy of GWO. ANN is a useful modeling technique because it can learn both linear and nonlinear relationships between variables. The neural network model that produces the fitness function for the system is developed using ANN.

ANN is applied with the GWO and other metaheuristic algorithms for many applications [36–38]. For instance, in [39], an ANN model is utilized in conjunction with the GWO for groundwater remedial design. The results are compared to the solutions of the ANN-PSO and ANN-Differential Evolution models, and it concluded that the suggested methodology has higher stability and convergence behavior. The study in [40] demonstrated the effectiveness of using the ANN-modified CSA-based approach to tune several PI controllers in a grid-connected photovoltaic system. In [41], ANN is combined with two

metaheuristic methods including GA and harmony search for weather forecasting. The graphical analysis and performance measurements revealed that the forecasting of daily mean temperatures has improved. In the article [42], an MPPT based on the artificial neural network was proposed to ensure that the system generated maximum power in variable atmospheric conditions. The obtained results demonstrated the superiority of the proposed method. In [43], a hybrid method, which combines both ANN & PSO for PV power generation was presented and showed that the ANN enables the existing PSO method to track MPP quickly.

However, a review of the literature found no evidence of GWO-ANN being utilized in the optimization gains of PI controllers of the DD-PMSG-VSWT study. In this paper, the GWO-ANN combination is utilized to fine-tune the PI regulators' gain factors employed within the GSI's vector control of the DD-PMSG-VSWT grid connection for the first time. The goal of this research is to come up with a solution to the improvement of the power quality as well as DC link voltage stability of grid-connected DD-PMSG-VSWT. The input errors to PI controllers are utilized as a fitness function. The GSI's sequential control contains three PI regulators. As a result, six parameters need to be optimized. The obtained results of the GWO-ANN provided DC link voltage stability and power quality performances. Section 2 provides a complete power system description. In Section 3, the GWO optimization and application procedures are introduced. Section 4, has shown simulation results and discusses them, and Section 5 is the conclusion.

## SYSTEM DESCRIPTION

The sub-parts of the model include a PMSG, wind turbine (WT), uncontrolled rectifier, boost converter, GSI, LCL filter, three-phase transformer, DC-link capacitor, grid, and transmission line as shown in Figure 1. The local AC load that has a 380V line-to-line voltage has been linked to a local AC bus. An LCL filter is put between the grid and the GSI for reducing the harmonics and improving the power quality. The mentioned local bus is linked to a three-phase 33 kV distribution grid using a 380V/33kV transformer. Table 1 shows the parameters of the considered system.

### Wind turbine model

In this model, WT transforms the wind's energy into mechanical power ( $P_m$ ), which is shown by the following relation regarding the changing wind speed ( $v_\omega$ ) [44]:

$$P_m = 0.5\ \rho A\ v_\omega^3\ c_P \tag{1}$$

In this case, $A$ shows the turbine's swept area $m^2$ , and $\rho$ shows the air density ( $kg/m^3$ ). $c_p$ the performance coefficient and it is a function of pitch angle ( $\beta$ ) and tip speed ratio ( $\lambda$ ) and is described as in (2)-(4):

$$c_p(\lambda,\beta) = c_1\left(\frac{c_2}{\lambda_i} - c_3\beta - c_4\right)\exp\left(\frac{-c_5}{\lambda_i}\right) + c_6\lambda \tag{2}$$

$$\frac{1}{\lambda_i} = \left(\frac{1}{\lambda + 0.08\beta} - \frac{0.035}{\beta^3 + 1}\right) \tag{3}$$

$$\lambda = r\,\omega / v_\omega \tag{4}$$

In this case, $\omega$ represents the rotational speed (rad/s) of blades while $r$ shows the blade radius (m). $c_1$, $c_2$ .... $c_6$ are constant coefficients, which depend on the blades' mechanical structure and their values are 0.5176, 116, 0.4, 5, 21, and 0.0068, respectively.

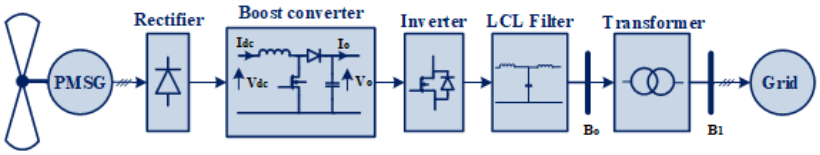


**Fig. 1.** WECS scheme utilizing a boost converter and a diode rectifier with a grid-side inverter

**Table 1.** Parameters of the system

| | |
|---|---|
| LCL filter parameters | $L_{inv}$ = 17 mH, C = 1.9 μF, $L_{grid}$ = 0.3 mH |
| Inverter output voltage | 380 V |
| Grid voltage | 33 kV |
| Frequency | 50 Hz |
| Load | 0.5 kΩ |
| DC-link voltage | 700 V |

### Generator-side converter

It controls the PMSG to get the MPPT operation. The MPPT operation is out of the scope of this study and another study describes it in detail [45].

### Grid-side Inverter

The GSI control system is used to regulate the d- and q-axis currents as well as the capacitor voltage. Figure 2 shows the outer loop of a GSI control for adjusting DC-link voltages. The grid current's quadratic component $i_q$ controls the reactive power. To assure a unity power factor, it must be set to zero. Grid voltage vector orientation control (VOC) is the foundation of the GSI control system.

VOC's grid side inverter control technique employs three control loops with PI controllers. The measured and transformed grid phase currents $i_d$ $i_q$ are compared to the reference grid currents $i^*_d$ and $i^*_q$. To achieve good control system attributes, special decoupling circuits are required, and they have been used in the control system. As a result, the active/reactive powers can be controlled directly through $i_d$ and $i_q$. The reference voltages $V_{q-ref}$ and $V_{d-ref}$ are later translated into systems a, b, and c before they are passed to the SPWM block.

## PROPOSED ALGORITHMS

### Artificial neural network

It is a data processing paradigm based on how the human nervous system sees and processes data. An artificial neural network (ANN) consists of finite artificial neurons that form an information network. The ANN models typically have an input and an output layer, having one or more hidden layers. One of the most often used ANNs is the feedforward neural network (FFNN). From the input layer, the data is first transmitted to hidden layers, which are later transmitted to the FFNN output layer. In any two layers of FFNN, the input-output data relationship can be mathematically stated as [39]:

$$y_j = f\left(\sum_{i=1}^{n} w_{ij} x_i + b_j\right) \qquad \begin{bmatrix} i = 1, 2, 3, \ldots\ldots n \\ j = 1, 2, 3, \ldots\ldots k \end{bmatrix} \tag{5}$$

Here, $k$ shows total neurons in an output/hidden layer, $n$ represents the total number of input-layer neurons, and $y_j$ shows the output value at the $j^{th}$ neuron. In this case, $x_j$ shows the input value at $j^{th}$ neuron, $b_j$ is the bias while $f$ shows the activation function and $w_{ij}$ shows the weight coefficients about input $x_i$ and output $y_j$. When an error function is minimized, ANN finds out the learnable parameters and $b_j$ optimal values, which have a batch of data. Here, the error function is expressed through mean squared error (MSE) [46]:

$$MSE = \frac{1}{m}\sum_{J=1}^{m}(y_j^p - y_j^a)^2 \tag{6}$$

In this case, $y_j^p$ shows the output data that ANN has predicted, while $m$ showing the total number of outputs, and $y_j^a$ is the real data.

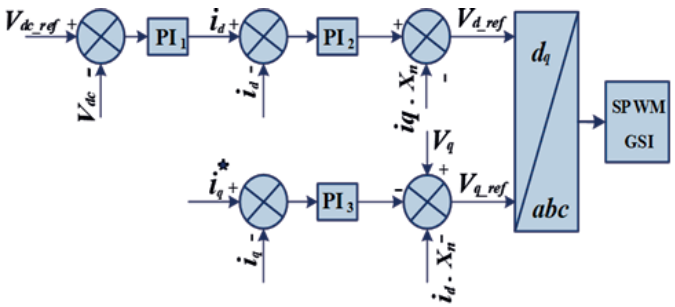


**Fig. 2.** The cascaded GSI control system

## Grey wolf optimization

In GWO, wolves are part of a pack and have exceptional hunting abilities. They also adhere to a strict social dominance hierarchy. This pack follows a tight dominance structure in which the group leader is Alpha (α) while the subordinates, called Beta ($\beta$), assist him and help him make decisions. As illustrated in Fig. 3, the remaining group members are either δ or ω. Alpha oversees deciding on a hunting target and directs Beta to join the hunt [47]. Beta follows Alpha's orders and informs the rest of the pack. Beta is also in charge of informing Alpha of all the pack's operations. Additionally, Beta may assist Alpha in deciding specific situations. Both Alpha and Beta wolves have authority over the third category of wolves, called delta wolves. Scouts, hunters, sentinels, caretakers, and elders are delta sub-types found in a typical pack. Omega is the pack's least dominant wolf, and to complete the hunt, they must follow Delta, Beta, and Alpha but Omega wolves are significant despite their lower hierarchical status. When Omega is not present, interns become irritable. Internal conflict in the pack emerges in the absence of omega, resulting in the breakdown of the social hierarchical structure. Wolves' hunting tactics include approaching, tracking, chasing, harassing, and encircling their prey, and when it stops moving, they attack it [48].

The encircling moves of the wolves are numerically approximated in a previous study [49]:

$$D = \left| C \times x_P(t) - x(t) \right| \tag{7}$$

$$x(t+1) = x_p(t+1) - A \times D \tag{8}$$

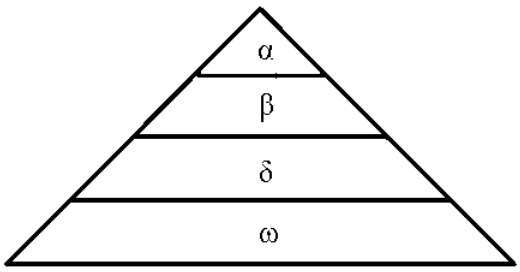


**Fig. 3.** Grey wolves' hierarchy

Here $x_p(t)$ shows the leading wolves' positions (positions of alpha, beta, or delta), $t$ is the present iteration, $x(t+1)$ is the arbitrary wolf's position in the iteration, and $x(t)$ is the arbitrary wolf's position, D shows the distance while A and C show coefficient vectors [50]:

$$\begin{gathered} A = (2r_1 - 1) \times a(t) \\ C = 2r_2 \\ a(t) = 2 - 2 \times t / T \qquad t = 1,2,3,.....T \end{gathered} \tag{9}$$

In this case, $r_1$ and $r_2$ are random values between [0, 1], $a(t)$ represents a variable with a linear iteration number reduced from 2 to 0, and T exhibits maximum iterations. If we take a look at the search area, Alpha has the ideal site to hunt his targets, which is followed by Beta, and Delta has the third position. All wolves (even Omega) acquired the top three places. The following set of equations can be used to depict a candidate wolf's position keeping in view the top three positions [51]:

$$\begin{aligned} D_\alpha &= \left| C \times x_\alpha(t) - x(t) \right| \\ D_\beta &= \left| C \times x_\beta(t) - x(t) \right| \\ D_\delta &= \left| C \times x_\delta(t) - x(t) \right| \end{aligned} \tag{10}$$

$$\begin{aligned} x_1(t+1) &= x_\alpha(t) - A \times D_\alpha \\ x_2(t+1) &= x_\beta(t) - A \times D_\beta \\ x_3(t+1) &= x_\delta(t) - A \times D_\delta \\ x(t+1) &= \frac{x_1(t+1) + x_2(t+1) + x_3(t+1)}{3} \end{aligned} \tag{11}$$

Here, $x(t)$ shows the candidate wolf's position, who takes the alternative positions $x_1(t+1), x_2(t+1), x_3(t+1)$ while $x_\alpha(t+1), x_\beta(t+1)$ and $x_\delta(t+1)$ represent the alpha, beta, and delta wolves' positions. Here $x(t+1)$ is the candidate wolf's position during the next iteration. The coefficients A and C in GWO are used to govern the search for space exploitation and exploration. The $|A| \geq 1$ value means that the wolves get the order to quit the current target. They will find the search space for selecting a suitable target. The $|A| \leq 1$ value directs how the wolves approach the target and catch it [52] as shown in Figure 4.

The reduction in the value of A is adaptively and stochastically concerned with iteration

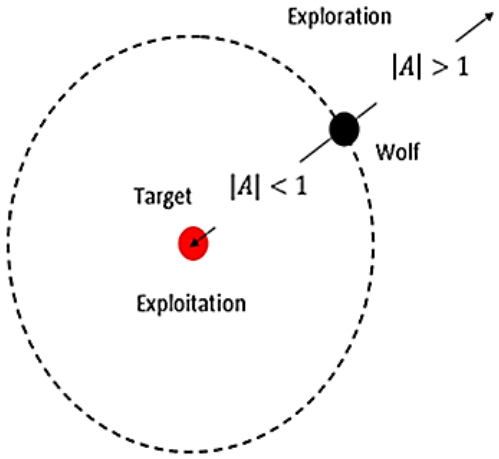


**Fig. 4.** Wolves' search space exploitation and exploration mechanisms [39]

numbers within the already known range [-2, 2] that creates an exploration-exploitation balance. The coefficient C has a uniform distribution, which is a random number in the range [0, 2]. In this case, C<1 is a stochastic variable that favors exploitation, whereas C>1 favors exploration. Here, coefficient C is independent of its iteration numbers while its stochastic behavior helps to avoid the local minima-trapping throughout the optimization process [53].

## Optimization procedure

First, MATLAB was used to create an ANN model through the DPGS model approximation. In addition, the ANN model is used in conjunction with GWO to achieve improvement goals. The model development technique is broken down into two steps:

*(i) Approximating the DPGS model with ANN*

- Dataset for input: The input dataset consists of the independent variables $[x_1, x_2, x_3, x_4, x_5, x_6]$ corresponding to the controller's gains and they can be represented as: $[K_{p1}, K_{i1}, K_{p2}, K_{i2}, K_{p3}, K_{i3}]$. The input dataset is produced at random within the controller's gains' minimum and maximum values.
- Dataset for output: It shows the dependent variables' values, which implement the standard deviation of errors $(e, e_1, e_2)$ according to the formula [54]:

$$\sigma = \sqrt{\frac{\sum (x_i - \mu)^2}{N}} \tag{12}$$

where: $\sigma$ = Set standard deviation,
$N$ = the size of the set,
$x_i$ = each value from the set,
$\mu$ = the set mean.

The output dataset is generated by executing 27 random runs to the DPGS model using the input dataset for 3.6s with 1 $\mu s$ sample time.

- Against the DPGS model, the ANN model is in the trained form and is evaluated by applying input/output datasets. The mean square error (MSE) and correlation coefficient are used to assess the ANN model's performance (R). Figures 5 and 6 demonstrate that the MSE values are closer to zero, and the correlation coefficient (R) is 1.

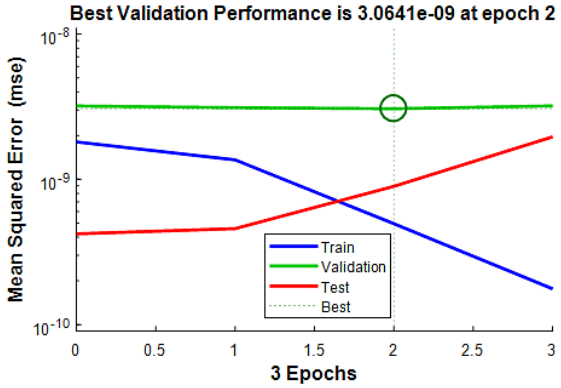


**Fig. 5.** Validation performance

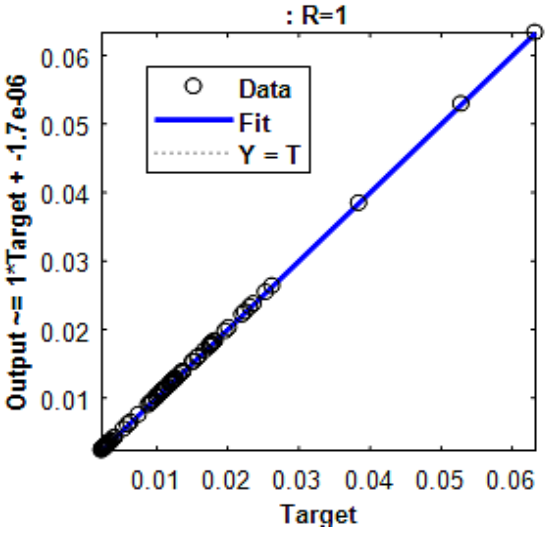


**Fig. 6.** Scatter plot depicting the relationship between ANN and DPGS output

*(ii) Coupled ANN-GWO model development*

- Initialize the positions of each wolf at random. The decision variable vector shows each wolf's position ($x$).
- Using the ANN model, calculate each wolf's fitness value ($F$).
- Three best values should be set as Alpha fitness ($F_\alpha$), beta fitness ($F_\beta$), and delta fitness ($F_\delta$).
- Assign the corresponding Alpha ($x_\alpha$), Beta ($x_\beta$), and Delta ($x_\delta$) to their corresponding positions.
- Using Eq. 9, calculate the coefficients $a$, $A$ and $C$ for each wolf ($x$).
- Using Eqs. 10 and 11, update each wolf's position.
- Steps 2–6 should be repeated until reaching the maximum iterations ($T$).

## Simulation Results and Discussion

The considered system's performance is examined through MATLAB/Simulink when there are wind speed variations, as given in Figure 7. PI controllers are adjusted according to the optimized gains by ANN-GWO, as Table 2 shows. After checking the controller's performance, the variable wind speed profile is applied to the DPGS.

**Table 2**. Optimized controller gains by the proposed method

| $K_{P1}$ | $K_{I1}$ | $K_{P2}$ | $K_{I2}$ | $K_{P3}$ | $K_{I3}$ |
|---|---|---|---|---|---|
| 10.87 | 478.42 | 1.809 | 3.905 | 1.382 | 3.638 |

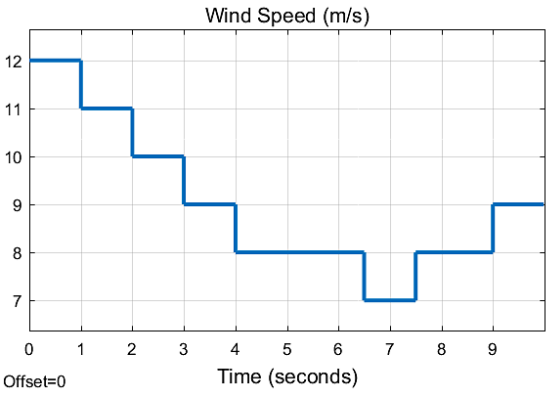


**Fig. 7.** Wind speed variation with time

As mentioned before, the DC bus reference voltage is 700 V and it should be almost the same for the control actions. Although the wind speed considerably changes, the bus voltage varies within the acceptable limits as illustrated in Figure 8. For the same wind profile, the fluctuations in the frequency have also been examined. It is obvious in Figure 9 that the wind speed variations usually cause slight frequency fluctuations. According to the IEC-61727 standard, the operating range is 50 ±1 Hz. It is concluded from Figure 9 that the fluctuation in frequency can be appropriate for the IEC-61727 standard.

For the grid-connected system, the smoothness of the voltages and currents is significant. At the inverter side and in the zoomed region, the 3-phase current/voltage is displayed in Figure 10. It is observed a small fluctuation in the voltage and current signals due to rapidly changing wind speed for a very short time (less than 1ms). The current increases as the wind speed increases and vice versa.

Figure 11 presents the clearer inverter current and output voltage signals for phase A. The phase voltage is smooth and steady-state. Also, it shows the matching of the voltage and current. Figure 12 shows the phase voltage A in waveforms both

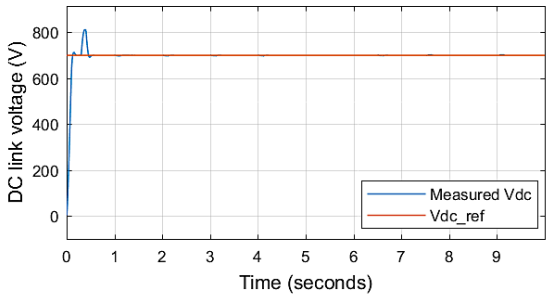


**Fig. 8.** DC link voltage (V)

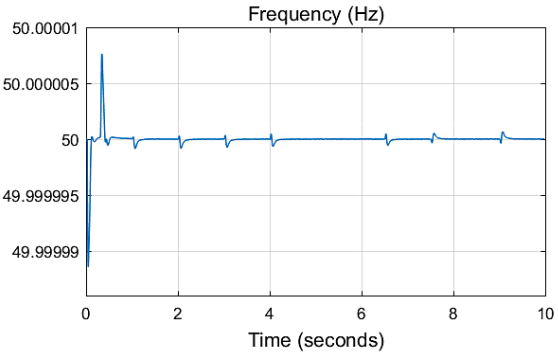


**Fig. 9.** Frequency of the injected power (Hz)

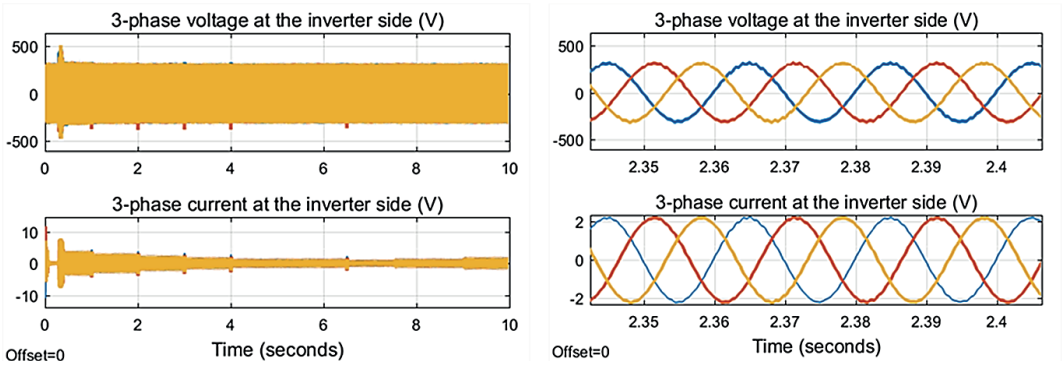


**Fig. 10.** (a) 3-phase current and voltage at the inverter side, (b) Zoomed current and voltage at the inverter side

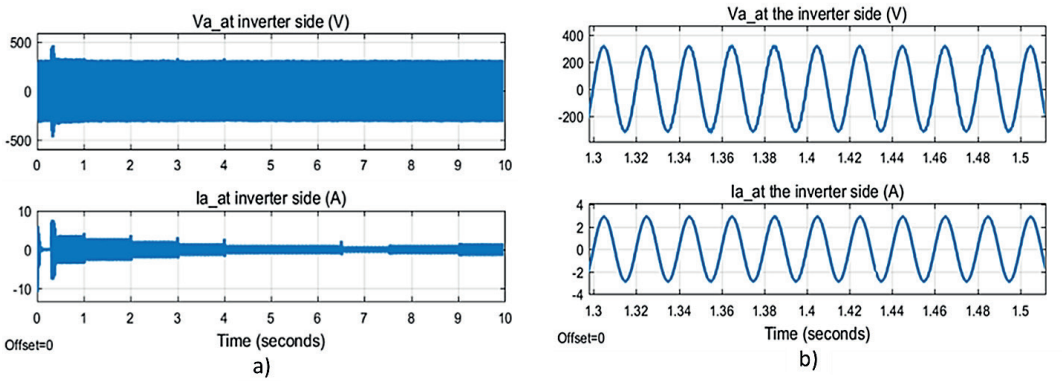


**Fig. 11.** (a) Phase A voltage and current at the inverter side, (b) Zoomed Phase A current and voltage at the inverter side

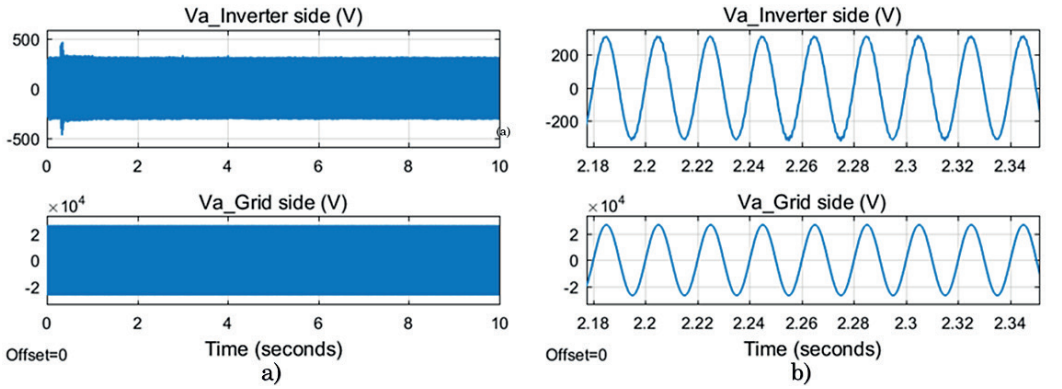


**Fig. 12.** (a) Phase voltage Va at the inverter and grid side, (b) zoomed region of Phase voltage Va at the inverter and grid side

for the inverter and the grid. It can be noticed that the waveforms are stable and they are in the same phase.

The voltage fluctuation of the RMS value of phase A is reserved within acceptable limits [55] regarding the inverter output nominal voltage ($V_{nom}$=220V) as illustrated in Figure 13. For THD, there is a standard (IEEE-519) and it must be less than 5% [56]. Figure 14 is given to examine THD for this study and it can be concluded from the same figure that the proposed controller assured the standard limit despite changing wind speed.

It is seen from Figure 14 that, the THD of the inverter voltage is 1.62% and the grid current is reduced to 0.93% with sinusoidal current injection into the grid.

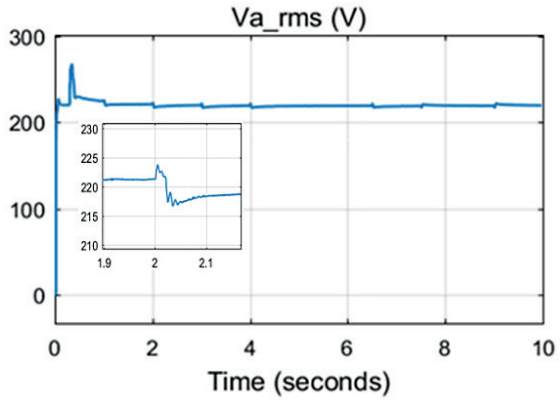


**Fig. 13.** RMS value of inverter voltage (phase A)

## CONCLUSIONS

This paper has proposed the ANN-based GWO algorithm for tuning the PI controllers' coefficients in the GSI of DPGS to improve the quality of power which is injected into the electric grid. The proposed GWO method has shown well-organized exploitation and exploration, and besides, it can avoid local optimum. Since this method is robust and simple, it can be applied to complex systems. Moreover, the proposed algorithm does not need any mathematical model. The ANN model is used as an alternative to DPGS. The ANN model is generated by using the range of the controllers' parameters as inputs and the standard deviation of the corresponding errors got previously by execution of the DPGS model. According to the ANN model's performance evaluation, the correlation coefficient (R) is one and the MSE is close to zero. Furthermore, because the ANN model is computationally effective, it is well-suited to the development of simulation-optimization systems. The ANN-GWO technique's influence can save time for parameter selection. It is proved from the results that the proposed method shows good performance in terms of the low THD, steady-state voltage, and frequency stability of the injected power by the WECS according to IEC standards despite changes in the wind speed. Therefore, it can be concluded that using an ANN-GWO-based strategy to tune multiple PI controllers in a grid-tied wind energy system is an effective method, and the procedure is also applicable to other power systems and renewable energy applications.

## REFERENCES

1. Yaylacı E, Yazici İ. Sensorless double integral sliding mode MPPT control for the WECS. J Renew Sustain Energy. 2018;10(2):023301.
2. Lee J, Zhao F. GWEC Global Wind Report. Glob Wind Energy Counc. 2022;75.
3. Gryniewicz-Jaworska M. Application of Heuristic Optimization for the Selection of Parameters of the Generation System and Reactive Power Consumption of Wind Farms. Adv Sci Technol Res J. 2020;14(3):9–14.
4. Bhadane K V, Jaware TH, Patil DP, Nayyar A. Wind Energy System Grid Integration and Grid Code Requirements of Wind Energy System. In Springer; 2021.
5. Ackermann T. Wind Power in Power Systems. Second Ed. John Wiley & Sons Ltd; 2012.
6. Nirosha C, Patra PSK. Power Quality Issues of Wind and Solar Energy Systems Integrated into the Grid. Adv Sci Lett. 2020;26(5):514–23.
7. Yaramasu V, Wu B. Model Predictiv Control of Wind Energy Conversion Systems. Hoboken, New Jersey: John Wiley & Sons, Inc.; 2017.
8. Eltamaly AM, Abdelaziz AY. Control and Op-

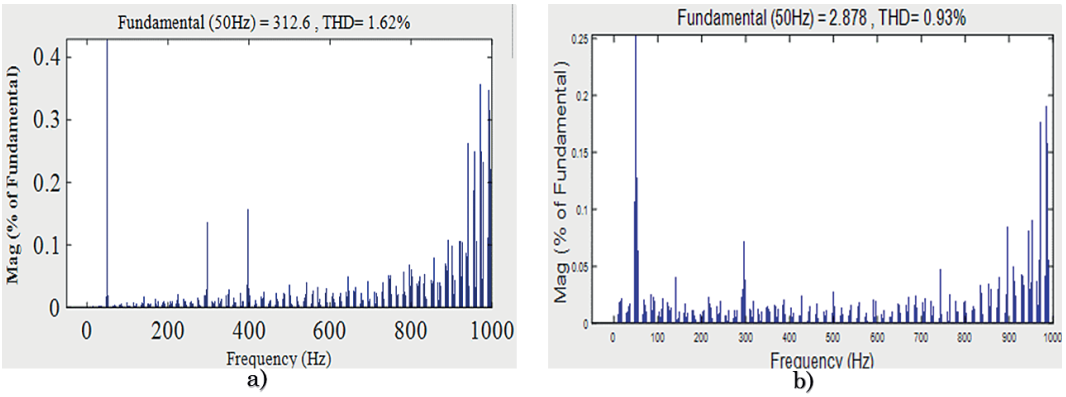


**Fig. 14.** (a) THD of voltage at the inverter side, (b) THD of current at the inverter side

eration of Grid-Connected Wind Energy Systems. Springer; 2021.

9. Oumaymah E. The injection of wind power into a grid using a multi-level inverter controlled by SVPWM. In: 4th International Conference on Electrical and Information Technologies ICEIT. Rabat, Morocco; 2020. p. 0–5.
10. Farh HMH, Eltamaly AM. Fuzzy Logic Control of Wind Energy Conversion System. J Renew Sustain Energy ·. 2013;5(2014):023125.
11. Li Z, Member S, Zang C, Zeng P, Yu H. Control of A Grid-Forming Inverter Based on Sliding Mode and Mixed H2 / H∞ Control. IEEE Trans Ind Electron. 2016;0046(c).
12. Errami Y, Ouassaid M, Maaroufi M. A performance comparison of a nonlinear and a linear control for grid connected PMSG wind energy conversion system. Int J Electr POWER ENERGY Syst. 2015;68:180–94.
13. Abdalrahman A, Zekry A. Control of the grid-connected inverter using dsPIC microcontroller. Proc 2013 2nd Int Japan-Egypt Conf Electron Commun Comput JEC-ECC 2013. 2013;(January 2014):159–64.
14. Wang Z, Qiu S, Song R, Wang X, Zhu B, Li B. Research on PID parameter tuning of coordinated control for ultra-supercritical units based on Ziegler Nichols method. IEEE. 2019;(Imcec):1155–8.
15. Przystupa K. Tuning of PID Controllers – Approximate Methods. Adv Sci Technol Res J. 2018;12(4):56–64.
16. Pajchrowski T, Zawirski K, Member S, Nowopolski K. Neural Speed Controller Trained Online by Means of Modified RPROP Algorithm. 560 IEEE Trans Ind INFORMATICS. 2015;11(April):560–8.
17. Hasanien HM, Member S, Muyeen SM, Member S. A Taguchi Approach for Optimum Design of Proportional-Integral Controllers in Cascaded Control Scheme. IEEE Trans Power Syst. 2012;(May 2013).
18. Joseph E, Olaiya OO. Cohen-coon PID Tuning Method ; A Better Option to Ziegler Nichols-PID Tuning Method. IJRERD. 2017;02(11):141–5.
19. Muyeen SM. An Affine Projection Algorithm based Adaptive Control Scheme for Operation of Variable-Speed Wind Generator. IET Gener Transm Distrib. 2015;9(August 2017):2611–6.
20. Agarwal J, Parmar G, Gupta R, Sikander A. Analysis of grey wolf optimizer based fractional order PID controller in speed control of DC motor. Microsyst Technol. 2018;24(12):4997–5006.
21. Qais MH, Hasanien HM, Alghuwainem S. A Grey Wolf Optimizer for Optimum Parameters of Multiple PI Controllers of a Grid-Connected PMSG Driven by Variable Speed Wind Turbine. IEEE. 2018; P 1.
22. Nicola M, Nicola CI. Improved Performance of Grid-Connected Photovoltaic System Based on Fractional-Order PI Controller and Particle Swarm optimization. Proc 2021 9th Int Conf Mod Power Syst MPS. 2021;(July):1–5.
23. Leandro B, Costa G, Bacon VD, Oliveira SA. Tuning of a PI-MR Controller Based on Differential Evolution Metaheuristic Applied to the Current Control Loop of a Shunt-APF. IEEE Trans Ind Electron. 2017;0046(c).
24. Durongdumrongchai P, Sa-Ngiamvibool W, Aurasopon A, Pothiya S. optimal fuzzy logic proportional integral derivative controllers design by bee algorithm for hydro-thermal system. Rev Roum des Sci Tech Ser Electrotech Energ. 2014;59(2):193–203.
25. Haridy AL. The Whale Optimization Algorithm based controller forfor PMSG wind energy generation system. 2019 Int Conf Innov Trends Comput Eng. 2019;(February):438–43.
26. Hasanien HM, Muyeen SM. Design optimization of controller parameters used in variable speed wind energy conversion system by genetic algorithms. IEEE Trans Sustain Energy. 2012;3(2):200–8.
27. Mirjalili S, Mirjalili SM, Lewis A. Grey Wolf Optimizer. Adv Eng Softw. 2014;69:46–61.
28. Faris H, Aljarah I, Azmi M, Mirjalili AS. Grey wolf optimizer : a review of recent variants and applications. Neural Comput Appl. 2017;30(July 2018):413–35.
29. Şen MA, Kalyoncu M. Optimal Tuning of PID Controller Using Grey Wolf Optimizer Algorithm for Quadruped Robot. Balk J Electr Comput Eng. 2018;6(1):29–35.
30. Kouba NEY, Menaa M, Hasni M, Boudour M. LFC enhancement concerning large wind power integration using new optimised PID controller and RFBs. IET Gener Transm Distrib. 2016;10(16):4065–77.
31. Yadav S, Verma SK, Nagar SK. Optimized PID controller for magnetic levitation system. IFAC-PapersOnLine. 2016;49(1):778–82.
32. Sule AH, Mokhtar AS, Bin Jamian JJ, Sheikh UU, Khidrani A. Grey Wolf Optimizer Tuned PI Controller for Enhancing Output Parameters of Fixed Speed Wind Turbine. 2020 IEEE Int Conf Autom Control Intell Syst I2CACIS 2020 – Proc. 2020;(June):118–22.
33. Osman A-SA, El-Wakeel AS, Kamel A, Seoudy HM, Osman, A. A. El-Wakeel, A. S., kamel, A., and Seoudy HM. Optimal tuning of PI Controllers for Doubly-Fed Induction Generator using Grey Wolf Optimizer. Int J Eng Res Appl. 2015;5(11):81–7.
34. Aguila-Leon J, Chinas-Palacios CD, Vargas-Salgado C, Hurtado-Perez E, Garcia EXM. Optimal PID Parameters Tunning for a DC-DC Boost Con-

verter: A Performance Comparative Using Grey Wolf Optimizer, Particle Swarm Optimization and Genetic Algorithms. In: IEEE Conference on Technologies for Sustainability,. Santa Ana, CA USA; 2020. p. 1–6.

35. Song X, Tang L, Zhao S, Zhang X, Li L, Huang J, et al. Grey Wolf Optimizer for parameter estimation in surface waves. Soil Dyn Earthq Eng. 2015;75:147–57.
36. Abdolrasol MGM, Hussain SMS, Ustun TS, Sarker MR, Hannan MA, , Ramizi Mohamed , Jamal Abd Ali, Saad Mekhilef AM. Artificial Neural Networks Based Optimization Techniques : A Review. Electronics. 2021;10(2689):43.
37. Raju P, Rao VM, Rao BP, Raju P, Rao VM, Rao BP. Grey Wolf optimization based Artificial Neural Network for Classification of Kidney Images. J Circuits, Syst Comput. 2018;27(14):1850231.
38. Hadavandi E, Mostafayi S, Soltani P. A Grey Wolf Optimizer-based Neural Network Coupled with Response Surface Method for Modeling the Strength of Siro-spun Yarn in Spinning Mills. Appl Soft Comput J. 2018;27(2018):1–13.
39. Majumder P, Eldho TI. Artificial Neural Network and Grey Wolf Optimizer Based Surrogate Simulation-Optimization Model for Groundwater Remediation. Water Resour Manag. 2020;34:763–83.
40. Kalaam RN, Muyeen SM, Al-Durra A, Hasanien HM, Al-Wahedi K. Optimisation of controller parameters for gridtied photovoltaic system at faulty network using artificial neural network-based cuckoo search algorithm. IET Renew Power Gener. 2017;11(12):1517–26.
41. Göçken M, Boru A, Dosdogru AT, Özçalici M. Integrating metaheuristics and artificial neural network for weather forecasting. Int J Glob Warm. 2018;14(4):440–61.
42. Gündoğdu A, Çelikel R. ANN-Based MPPT Algorithm for Photovoltaic Systems. Turkish J Sci Technol. 2020;15(2):101–10.
43. Rahman M, Islam S. PSO and ANN Based Hybrid MPPT Algorithm for Photovoltaic Array under Partial Shading Condition. Eng Int. 2020;8(1):9–24.
44. Yazıcı İ, Yaylacı EK, Yalçın F. Modified golden section search based MPPT algorithm for the WECS. Eng Sci Technol an Int J. 2021;24(5):1123–33.
45. Yazici I, Yaylaci EK, Cevher B, Yalçln F, Yüzkollar C. A new MPPT method based on a modified Fibonacci search algorithm for wind energy conversion systems. J Renew Sustain Energy. 2021;13(1):013304.
46. Moghdani S and. A Hybrid Artificial Neural Network with Metaheuristic Algorithms for Predicting Stock Price. Cybern Syst AN Int J. 2017;9722(March):0–28.
47. Chapter B. Advanced Optimization by Nature-Inspired Algorithms. Studies in Computational Intelligence. Springer; 2018.
48. Bansal JC, Singh S. A better exploration strategy in Grey Wolf Optimizer. J Ambient Intell Humaniz Comput. 2021;12(1):1099–118.
49. Dada E, Joseph S, Oyewola D, Fadeel A, Chiroma H, Abdulhamid S. Application of Grey Wolf Optimization Algorithm: Recent Trends, Issues, and Possible Horizons. Gazi Univ J Sci. 2021;35(2):485–504.
50. Sulaiman MH, Mustaffa Z, Mohamed MR, Aliman O. Using the gray wolf optimizer for solving optimal reactive power dispatch problem. Appl Soft Comput J. 2015;32:286–92.
51. Hassan HA, Zellagui M. Application of grey wolf optimizer algorithm for optimal power flow of two-terminal HVDC transmission system. Adv Electr Electron Eng. 2017;15(5):701–11.
52. Sezer K, Bayhan N. Comparison of Metaheuristic Algorithm Performances for Optimization of Fractional Order PID Controllers Applied to Gas Turbine Power Plant. Aeronaut Sp Technol. 2021;14(2):209–19.
53. Kamal S, Rani S, Rattan DM. Review of Grey Wolf Optimizer and Its Applications. Int J Eng Appl Sci Technol. 2020;04(11):208–11.
54. Schiefer H, Schiefer F. Statistics for Engineers An Introduction with Examples from Practice. springer. 2021.
55. Mohod SW, Aware M V. Power Quality and Grid Code Issues in Wind Energy Conversion System. In InTech; 2013.
56. Saïd-Romdhane M Ben, Naouar MW, Belkhodja IS, Monmasson E. Simple and systematic LCL filter design for three-phase grid-connected power converters. Math Comput Simul. 2016;130:181–93.